

UC Irvine

UC Irvine Previously Published Works

Title

A new approach to studying aqueous reactions using diffuse reflectance infrared Fourier transform spectrometry: application to the uptake and oxidation of SO₂ on OH-processed model sea salt aerosol.

Permalink

<https://escholarship.org/uc/item/5dz6b2kv>

Journal

Physical chemistry chemical physics : PCCP, 9(16)

ISSN

1463-9076

Authors

Shaka', Huda
Robertson, W H
Finlayson-Pitts, Barbara J

Publication Date

2007-04-28

Peer reviewed

A new approach to studying aqueous reactions using diffuse reflectance infrared Fourier transform spectrometry: application to the uptake and oxidation of SO₂ on OH-processed model sea salt aerosol†

Huda Shaka', W. H. Robertson and Barbara J. Finlayson-Pitts*

Received 1st September 2006, Accepted 29th January 2007

First published as an Advance Article on the web 27th February 2007

DOI: 10.1039/b612624c

Diffuse reflectance infrared Fourier transform spectrometry (DRIFTS) is a powerful technique for analyzing solid powders and for following their reactions in real time. We demonstrate that it can also be applied to studying the uptake and reactions of gases in liquid films. Within the DRIFTS cell, a 10% (w/w) mixture of MgCl₂ · 6H₂O in NaCl was equilibrated with air at 50% RH, which is above the deliquescence point of the magnesium salt but below that of NaCl. This mixture of NaCl coated with an aqueous magnesium chloride solution was then reacted with gas phase OH to generate hydroxide ions *via* a previously identified interface reaction. This treatment, hereafter referred to as OH-processing, was sufficient to convert some of the magnesium chloride to Mg(OH)₂ and Mg₂(OH)₃Cl · 4H₂O, making the aqueous film basic and providing a reservoir of alkalinity. Subsequent addition of SO₂ to the basic processed mixture resulted in its uptake and conversion to sulfite which was measured by FTIR. The sulfite was simultaneously oxidized to sulfate by HOCl/OCl⁻ that was formed in the initial OH-processing of the salt. Further uptake and oxidation of SO₂ in the aqueous film took place when the salt was subsequently exposed to O₃. These studies demonstrate that DRIFTS can be used to study the chemistry in liquid films in real time, and are consistent with the hypothesis that the reaction of gaseous OH with chloride ions generates alkalinity that enhances the uptake and oxidation of SO₂ under these laboratory conditions.

1. Introduction

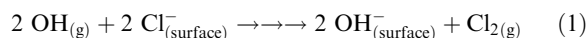
A number of reactions of gases at water interfaces and in thin aqueous films on solids have been previously reported.^{1–15} These are interesting and important both from the point of view of fundamental physical chemistry and in terms of their application to such fields as atmospheric chemistry. Chemistry at air–water interfaces is likely to be particularly important for airborne particles which have large surface-to-volume ratios. However, studying the uptake and reactions of gases occurring in and on suspended liquid aerosol particles in real time is difficult.

A variety of methods that have been applied are reviewed in detail elsewhere.¹⁶ For example, for large (~10 μm) size particles, the falling droplet apparatus has been used extensively to study gas uptake and reaction.^{1,3,13,17,18} FTIR studies of smaller particles have been carried out at relatively high particle concentrations;^{19–22} following the particles with time using this method is complicated by continuously changing particle size distributions due to coagulation and settling of the particles.^{23,24} A new technique is optical levitation of single droplets combined with Raman spectroscopy, but this has only been applied to relatively few systems to date.^{25–27} Single

particle mass spectrometry is another promising technique for the study of chemistry on aerosols; but in addition to the instrumental costs, the different approaches used for volatilization and ionization result in variable sensitivities for different components. In addition, extensive fragmentation, particularly of organics, makes speciation difficult or impossible.^{28–34}

Diffuse reflectance infrared Fourier transform spectrometry (DRIFTS) is a powerful technique for following the chemistry of solid particles in real time under laboratory conditions.^{35–38} It has the advantage of relatively strong signals due to the macroscopic amounts of sample used, but the matrix used must be infrared transparent. DRIFTS is not normally applicable to liquids where interface and bulk liquid phase reactions are important. However, we demonstrate here that for appropriate systems, DRIFTS can indeed be used to study reactions in and on thin aqueous films on solid substrate powders.

An interface reaction of particular relevance to the current work is that of gas phase OH with chloride ions at the surface of sea-salt aerosols.^{7,39,40}



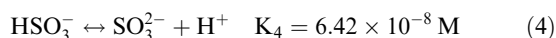
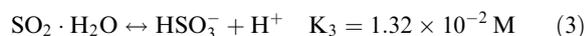
This represents the overall reaction since the individual steps of the mechanism are not well known. It is important to note that this reaction only occurs at the interface of aqueous solutions containing chloride ions; no such reaction has been observed either in bulk solutions or with solid NaCl.^{7,39,41} Reaction (1) has some unique features compared to the bulk phase oxidation of chloride.^{42,43} First, because it takes place at

Department of Chemistry, University of California Irvine, Irvine, CA 92697-2025, USA. E-mail: bfinlay@uci.edu; Fax: (949) 824-3168; Tel: (949) 824-7670

† Electronic supplementary information (ESI) available: Reactions used in kinetics modeling of O₃ photolysis. See DOI: 10.1039/b612624c

the interface, OH need not be taken up into the liquid phase before reacting. This increases the rate of chloride oxidation because the reaction is not limited by mass accommodation or by the solubility of OH in solution. Indeed, a lower limit for the reaction probability of gas phase OH with chloride ions at the surface of deliquesced NaCl particles has been measured recently to be $\gamma > 0.1$.⁴⁴ Second, reaction (1) does not require acid, but actually generates base as reported by Laskin *et al.*⁴⁰ based on TOF-SIMS and SEM-EDX data. They proposed that this reaction could indirectly impact the uptake and oxidation of SO₂ to sulfate in sea-salt aerosols by maintaining an alkaline pH longer than would be the case without this chemistry.

In the marine boundary layer (MBL), airborne sea-salt particles generated by wave action^{45–47} provide an important pathway for SO₂ oxidation. They are believed to contribute significantly to the removal of SO₂ from the MBL and to the formation of sulfate,^{48–73} which impacts radiative forcing and global climate.^{66,74–79} Fresh sea-salt particles are buffered at an alkaline pH, which promotes the uptake of SO₂ *via* reactions (2)–(4):⁸⁰



Through these equilibria, the total amount of dissolved S(IV) (defined as S(IV) = SO₂·H₂O + HSO₃[−] + SO₃^{2−}) increases with increasing pH. Dissolved S(IV) is oxidized in the aqueous phase and on the surfaces of particles by a number of oxidants, such as H₂O₂, O₃, HOCl, HOBr and O₂ catalyzed by metals and perhaps by chloride ions.^{50–55,57,60,71,81–95} SO₂ can also be oxidized in the gas phase, mainly by OH,⁹⁶ to produce sulfuric acid which is then taken up by cloud droplets and particles; however, this is generally a minor pathway compared to aqueous oxidation.¹⁶

In this work, we demonstrate the application of DRIFTS to studying the uptake and oxidation of gaseous SO₂ at 50% relative humidity (RH) on NaCl–MgCl₂·6H₂O salt mixtures that have been previously reacted with OH formed by the photolysis of O₃ in the presence of water vapor. Because reaction (1) generates base, it is expected to increase the uptake of SO₂ as well as its oxidation by ozone which is particularly important above a pH of ~ 6.^{50,53–55,60,82,87}

At 50% RH, a mixture of NaCl with MgCl₂·6H₂O consists of a saturated solution of MgCl₂·6H₂O (deliquescence relative humidity, DRH, is 33%) with some dissolved NaCl in contact with solid NaCl (DRH is 75%).⁹⁷ The deliquesced magnesium chloride provides the aqueous film required for the chemistry to occur, and the undissolved NaCl powder permits the application of DRIFTS. Some transmission-FTIR experiments on deliquesced particles in an aerosol chamber and attenuated total reflectance FTIR (ATR-FTIR) experiments on bulk solutions were also carried out to confirm the DRIFTS band assignments and to probe some aspects of the chemistry that were not experimentally accessible using DRIFTS. We show that OH processing of this model for sea salt increases the uptake of SO₂ and that oxidation to sulfate occurs initially without the addition of O₃. Additional oxidation by the S(IV) + O₃ reaction occurs subsequently. The mechanisms and implications for sea salt chemistry are discussed.

2. Experimental

The DRIFTS apparatus^{36,98} is shown in Fig. 1. Briefly, the system consisted of a diffuse reflectance accessory in a vacuum chamber (Harrick Model HVC2-DR2) with CaF₂ windows (Harrick Scientific-Model DRA-2CS) and housed in a Mattson RS FTIR spectrometer. The bottom of the sampling cup is open to a vacuum pump but covered with a screen to hold the salt sample while permitting pumping of gases through the salt. The sample cell has a volume of 11 cm³ and was water-cooled throughout the experiment to minimize heating of the salt during irradiation.

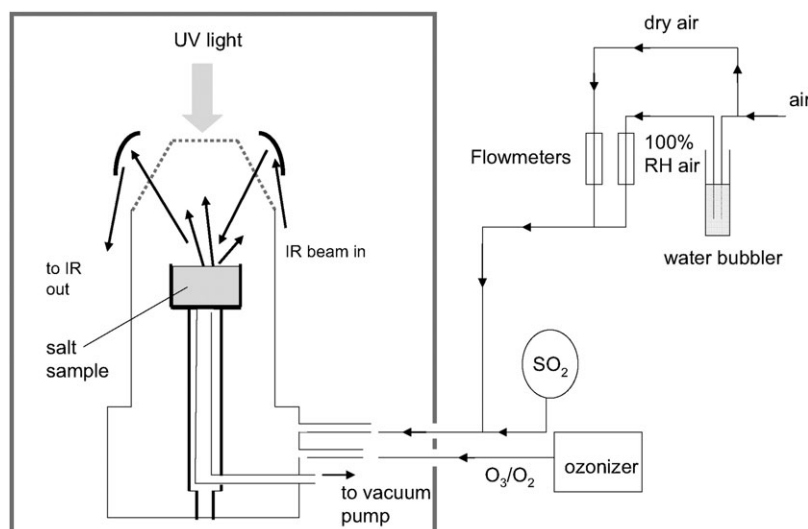


Fig. 1 Schematic of DRIFTS apparatus and flow system.

DRIFTS requires the use of a solid powder in which the infrared beam undergoes multiple scattering while light is absorbed by infrared active components.³⁵ Liquid and gaseous samples cannot be studied with this technique, although gases can be measured if they are present at sufficiently high concentrations to be measurable at the short total pathlength (~ 3 cm) between the CaF_2 windows and the salt sample. The reactions of interest in this experiment require the presence of at least a thin quasi-liquid layer on the salt sample. Thus, a mixture of sodium chloride and hygroscopic magnesium chloride salts was used to satisfy both requirements, as will be discussed further in the next section. In addition, the mixture of sodium and magnesium chloride provides a more realistic proxy of sea-salt than pure NaCl , since MgCl_2 is the second most abundant component of sea-salt after NaCl . Seawater has a molar ratio of MgCl_2 to NaCl of 0.13.⁹⁹ A smaller fraction of the magnesium salt (0.03) was used here for ease of sample handling and obtaining useful DRIFTS spectra, which becomes more difficult as the water content of the sample increases.

The salt mixture was prepared by grinding 0.27 g of NaCl crystals (Fischer, ACS grade) with 0.03 g of dry $\text{MgCl}_2 \cdot 6\text{H}_2\text{O}$ (Sigma Chemicals, ACS grade) in a Wig-L-Bug (Crescent Dental Manufacturing Company) for 5 min. It was necessary to dry both the NaCl and $\text{MgCl}_2 \cdot 6\text{H}_2\text{O}$ before grinding to avoid clumping of the salts in the Wig-L-Bug. NaCl was oven dried. However, $\text{MgCl}_2 \cdot 6\text{H}_2\text{O}$, which is highly hygroscopic, could not be treated the same way because it is known to dehydrate upon heating to produce $\text{Mg}(\text{OH})\text{Cl}$ and MgO .^{100,101} To remove adsorbed water on the $\text{MgCl}_2 \cdot 6\text{H}_2\text{O}$, the salt was pumped on at room temperature for an hour using a conventional vacuum system ($\sim 10^{-5}$ Torr). Samples that were heated in an oven or pumped overnight gave cloudy solutions in water, indicating the presence of $\text{Mg}(\text{OH})\text{Cl}$ or MgO . However, $\text{MgCl}_2 \cdot 6\text{H}_2\text{O}$ that had been pumped for only one hour gave a clear solution, indicating insignificant decomposition of the salt.

To characterize the morphology and elemental composition of the salt mixtures, an FEI/Philips XL-30 Schottky thermal field emission scanning electron microscope (SEM) coupled to an EDAX energy dispersive X-ray spectrometer (EDS) was used. The SEM and EDS data were collected at a pressure of $\sim 10^{-5}$ Torr using an accelerating beam voltage of 10 kV and magnifications between 5000 and 15 500. The SEM images were collected using the secondary electron detector.

In a typical DRIFTS experiment, the 0.30 g salt mixture of $\text{NaCl-MgCl}_2 \cdot 6\text{H}_2\text{O}$ was processed sequentially in the following manner (details given below): (1) the salt sample was equilibrated at a relative humidity of $\sim 50\%$, and then exposed to OH radicals produced from the UV photolysis of O_3 (salt treated this way is hereafter referred to as OH-processed); (2) gaseous SO_2 was introduced into the cell in the dark with the RH maintained at $\sim 50\%$, and its uptake and oxidation products in the salt (sulfite and sulfate) monitored over a period of time using DRIFTS; (3) gaseous O_3/O_2 was introduced to the cell in the dark so that the OH-processed salt was exposed to both SO_2 and O_3 simultaneously, again at an RH of $\sim 50\%$. The relative humidities were calculated from the cell pressure and the measured flow rates of the

gases. All gas exposures were carried out in the flow mode with gases being pumped through the salt. DRIFTS spectra were collected at all stages of the experiment, except during photolysis, using 16 cm^{-1} resolution and 512 scans per spectrum.

The total pressure and relative humidity in the cell were controlled using a valve between the cell and the pump and by adjusting the relative flows of water-saturated air, SO_2/N_2 and O_3/O_2 . The air used was Scott-Marrin (Ultra Pure, <0.01 ppm total hydrocarbons (as CH_4), <0.01 ppm CO , <0.001 ppm NO_x , <0.001 ppm SO_2 , <2 ppm CO_2). The salt sample was allowed to equilibrate with the humidified air (50% RH) for an hour at a total pressure of 0.5 atm. A mixture of 2.8% O_3/O_2 (Oxygen Services Company Ultra High Purity, $>99.999\%$) produced by electric discharge using a commercial ozonizer (Polymetrics Ozone Generator, Model-T816) was then added to give a total pressure of 1 atm. The total flow was $48 \text{ cm}^3 \text{ min}^{-1}$ and the ozone concentration was 3×10^{17} molecules cm^{-3} . The flowing gas mixture in the cell was then irradiated for two hours using a high pressure 200 W Hg lamp (Spectra Physics, power supply Model 69907, lamp housing Model 66902) that had a 10 cm water filter with quartz windows ($\lambda > 200$ nm) located between the lamp and DRIFTS cell to absorb infrared radiation and minimize heating of the sample. The temperature rise of the cell during photolysis was typically 3–4 °C.

The photolysis of O_3 below 350 nm forms $\text{O}(^1\text{D})^{16}$ which reacts with water vapor to generate gaseous OH. Secondary chemistry (ESI^\dagger) generates additional species such as HO_2 and H_2O_2 . The concentrations of the gas phase species were calculated using a numerical integration program, Acuchem.¹⁰² Except for the photolysis rate constants (k_p) for O_3 and H_2O_2 , all of the gas phase rate constants are known.^{103,104} The value of k_p for O_3 was determined in independent static experiments in which the loss of O_3 during photolysis in the DRIFTS cell was followed at 47% RH using its gas phase absorbance at 1028 cm^{-1} . The value of k_p used as input to the Acuchem model was varied to fit the measured decay of O_3 , giving $k_p = 5 \times 10^{-5} \text{ s}^{-1}$. This gas phase modeling predicts a steady-state gas phase OH concentration of $1 \times 10^{10} \text{ OH cm}^{-3}$ after 14 s of photolysis (the average residence time of gases in the cell) if there was no loss of OH or other intermediates and products to the walls or from uptake and reaction with the salt.

After photolysis, the O_3/O_2 flow was stopped and the sample was given time to re-equilibrate (~ 1 hr) to insure that the temperature and relative humidity returned to the initial, pre-photolysis values. Gaseous SO_2 (Matheson Gas Products, 99.98%) diluted 1 : 100 with N_2 (Oxygen Services Company, Ultra High purity, $>99.999\%$) was then flowed through the cell to give an SO_2 concentration of 4.8×10^{15} molecule cm^{-3} at an RH of 50% and a total pressure of 391 Torr. It is important that SO_2 not be introduced during irradiation in order to prevent its direct oxidation by OH. Subsequently, O_3/O_2 was added to the DRIFTS cell in the dark, and the flows and pumping adjusted to give a total pressure of 474 Torr, an RH of 52%, an ozone concentration of $4.0 \times 10^{16} \text{ cm}^{-3}$ and an SO_2 concentration of $1.3 \times 10^{16} \text{ cm}^{-3}$. Sulfate formation was again monitored using FTIR.

In order to quantify the amount of sulfate formed in the salt, the 0.30 g salt sample was dissolved in 25.0 mL of Nanopure[®] water (Barnstead 18 M Ω cm) for analysis by ion chromatography (IC) using a conductivity detector (Alltech, Allsep A-2 Anion IC column). The mobile phase was 1.7 mM NaHCO₃–1.8 mM Na₂CO₃ buffer solution, prepared from a concentrated Alltech EZ-LUTE solution. The IC system was calibrated using Na₂SO₄ solutions at varying concentrations, prepared from a standard Na₂SO₄ solution supplied by the manufacturer.

As mentioned above, DRIFTS can only be applied to solid powders, but some of the chemistry occurring in the thin water film on the particles involves species such as OCl[–] that are not stable as solids. In order to probe this chemistry and to obtain reference spectra of SO₃^{2–} and SO₄^{2–} in solution for comparison to the DRIFTS spectra, chamber experiments on aerosols were carried out. A detailed description of the aerosol chamber can be found in Ramazan *et al.*¹⁴ Briefly, it consists of a cylindrical borosilicate cell that is 30 cm in diameter and 1.2 m in length with stainless steel endplates that hold infrared reflective mirrors in a White cell configuration.¹⁰⁵ The total volume of the chamber is 102 L. The path length was set at 47.8 m, allowing both gas phase and aerosol components to be interrogated using infrared spectroscopy. These experiments were conducted at a relative humidity between 60 and 90% and a temperature of 298 \pm 3 K.

Aerosols were produced using a TSI Atomizer (Model 3076) and were then directly introduced into the chamber. NaOCl aerosols were atomized from a 0.05% (w/v) aqueous solution of NaOCl reagent (prepared from Spectrum NaOCl ACS reagent, min. 5% chlorine). NaCl aerosols were atomized from a 1% (w/v) aqueous solution of NaCl. The particle size distribution for the NaCl aerosols was characterized using a TSI scanning mobility particle sizer (SMPS) consisting of an electrostatic classifier (Model 3080) equipped with a differential mobility analyzer (DMA, Model 3081) and a condensation particle counter (CPC, Model 3022A). Typical NaCl aerosol concentrations in these experiments were 8 \times 10⁵ particles cm^{–3} with a geometric mean diameter of 130 nm (σ_g = 1.40).

In order to obtain a calibration for the sulfite infrared peak, a bulk aqueous solution of 0.7 M Na₂SO₃ was prepared and the spectrum of the solution obtained by placing a few drops of it on top of an ATR crystal. A Jasco 615 FTIR spectrometer was used with a PIKE single-bounce ATR accessory. In this case, no sulfate was observed. The solution was then oxidized by bubbling O₃/O₂ through the solution and withdrawing aliquots at various times for analysis until the sulfite had been completely converted to sulfate. This allowed the relative infrared absorption cross sections for sulfite and sulfate to be obtained, assuming a 1 : 1 relationship between sulfite reacted and sulfate formed.

3. Results and discussion

Characterizing the reactant mixture

Fig. 2 shows an SEM image of a typical NaCl–MgCl₂·6H₂O salt sample. A typical particle diameter is \sim 1 μ m. EDS analysis showed that the Na : Mg ratio over four different

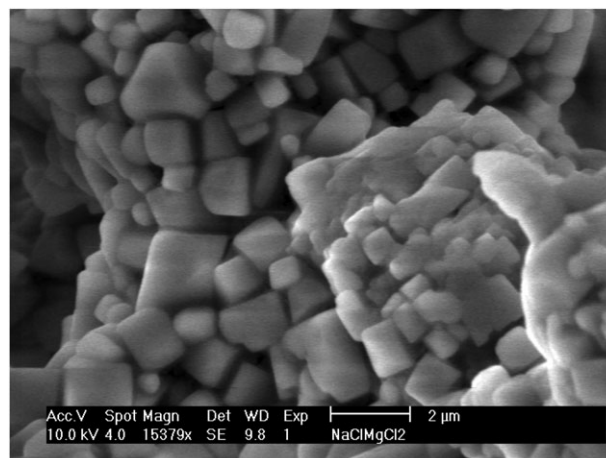


Fig. 2 SEM image of an NaCl–MgCl₂·6H₂O (9 : 1 w/w) salt sample that had been mixed in a Wig-L-Bug. Beam voltage was 10.0 kV, magnification was 15 000. Sample chamber was at \sim 10^{–7} Torr.

500–600 μ m² areas averaged 33 \pm 3 (1 σ), which is in excellent agreement with the ratio of 31 expected for 0.27 g NaCl mixed with 0.03 g MgCl₂·6H₂O. Scans of smaller sample areas gave a higher variability, indicative of some heterogeneity in the distribution of the magnesium chloride.

The deliquescence points of MgCl₂·6H₂O and NaCl at 298 K are 33% and 75%, respectively.¹⁰⁶ Because MgCl₂·6H₂O has waters of hydration and likely some adsorbed water as well, it is a ‘soft’ salt that is expected to coat the NaCl particles at least in part during the grinding process. Once the salt sample is in the DRIFTS apparatus, the RH is raised to 50% which will dissolve the magnesium chloride and allow it to coat the NaCl. Tang⁹⁷ has measured the properties of mixtures of MgCl₂·6H₂O and NaCl and has shown that at 50% RH, the equilibrium solution consists of magnesium chloride (4.2 molal), smaller amounts of dissolved NaCl (0.6 molal) and solid NaCl. Based on these concentrations and the SEM/EDS results, the NaCl–MgCl₂·6H₂O samples in the DRIFTS cell at 50% RH are considered as consisting of a solid core of NaCl particles coated by a solution of MgCl₂ with smaller amounts of dissolved NaCl. Based on the thermodynamic calculations of Tang,⁹⁷ the initial volume of solution associated with the particles at 50% RH is 0.04 cm³ for the 0.30 g samples used in these experiments.

OH processing of the samples, and uptake and initial oxidation of SO₂

DRIFTS spectra obtained from NaCl–MgCl₂·6H₂O salt samples exposed to the O₃/H₂O photolysis intermediates and products, including OH, followed by the addition of SO₂ are shown in Fig. 3. The numbers on the spectra indicate the time elapsed from the beginning of SO₂ addition. The dotted trace in Fig. 3 shows the spectrum obtained 3 min after SO₂ was added to a sample that had been OH-processed for 2 h. Initially, a peak appears at \sim 955 cm^{–1} that is attributable¹⁰⁷ to sulfite, SO₃^{2–}. With time, this peak decreases while another peak grows in at 1106 cm^{–1} and is assigned to sulfate (SO₄^{2–}).¹⁰⁷

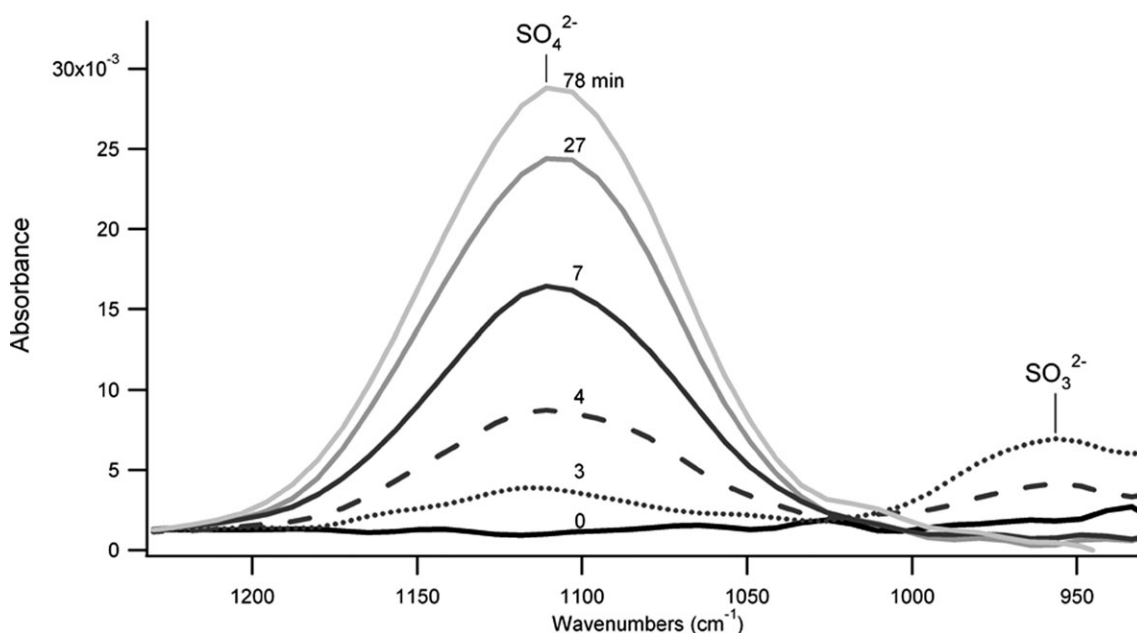


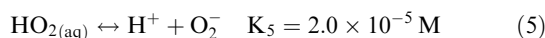
Fig. 3 DRIFTS spectra of an OH-processed (2 h exposure) NaCl-MgCl₂·6H₂O salt sample at 50% RH and 391 Torr total pressure upon addition of 4.8×10^{15} molecule cm⁻³ SO₂. The numbers on the spectra indicate the time elapsed (in minutes) from the beginning of SO₂ exposure.

Control experiments were carried out in which the unprocessed salt was exposed to SO₂; neither sulfite nor sulfate were formed. In addition, no sulfite or sulfate were observed after SO₂ was added to a salt sample that had been exposed to UV in the absence of O₃, nor in one which had been exposed to O₃ in the absence of UV.

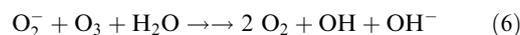
In short, the salt must be OH-processed for measurable amounts of sulfite and sulfate to be formed, consistent with increased alkalinity of the processed salt due to reaction (1) and the increased solubility of SO₂ at high pH. The absence of the bisulfite peak¹⁰⁷ at 1023 cm⁻¹ in Fig. 3 is another indication of the alkalinity of the salt sample. Note that reaction (1) does not occur if the chloride is in a solid salt, confirming that the chemistry must be occurring in an aqueous film on the salt. These observations are consistent with Raman spectroscopy studies of Aardahl and Davis¹⁰⁸ which showed sulfite formation upon uptake of gaseous SO₂ into aqueous NaOH aerosols.

Altmaier *et al.*¹⁰⁹ have shown that Mg(OH)₂ reacts to form the Mg₂(OH)₃Cl·4H₂O (hydroxychloride) in magnesium chloride solutions with concentrations greater than 2 molal. The *K*_{sp} for magnesium hydroxide is 1.25×10^{-11} at 25 °C.¹¹⁰ This implies that as the aqueous film becomes increasingly basic during the OH reaction with chloride ions, hydroxide ions will become sequestered as solid Mg(OH)₂ and then as Mg₂(OH)₃Cl·4H₂O. Another potential contributor to sequestering base is the uptake of CO₂ and formation of magnesium carbonate. The levels of CO₂ in the air used for the experiments were small, 2 ppm or less, so that this is not expected to be a major contributor. In any case, hydroxide is sequestered in these salts and is available to neutralize SO₂ as it is taken up and oxidized to sulfate. The solubility¹¹¹ of Mg₂(OH)₃Cl·4H₂O is such that it requires lower pH values to dissolve this salt compared to Mg(OH)₂. It is thus expected that the hydroxide will dissolve first as acid is generated by the sulfite oxidation, followed by dissolution of Mg₂(OH)₃Cl·4H₂O.

There is an additional source of OH in the salt samples that must be considered. Secondary chemistry during the O₃/H₂O photolysis generates other intermediates and products (supplementary information) including HO₂ which in solution is a weak acid:

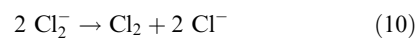
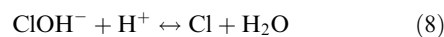


In the presence of ozone, O₂⁻ undergoes an electron transfer to O₃, which in the presence of water reacts to form OH:



The net result is the reaction of HO₂ in bulk solution to generate OH. Taking Henry's Law constants¹¹² for HO₂ and O₃ of 5.7×10^3 and 1.1×10^{-2} M atm⁻¹, respectively, the aqueous phase equilibrium concentrations of HO₂ and O₃ after 14 s photolysis in the absence of reaction with the salt are predicted to be 7.1×10^{-5} M and 1.4×10^{-4} M. At a pH of 7, the equilibrium concentration of O₂⁻ in the absence of further reaction would be 1.4×10^{-2} M, and larger at basic pH. If the rate of electron transfer from O₂⁻ to O₃ is rate determining ($k = 1.52 \times 10^9$ M⁻¹ s⁻¹),¹¹³ then this source of OH will overwhelm that due to the uptake of OH from the gas phase.

However, it is important to note that reactions (5) and (6) will generate OH in the bulk aqueous phase where not only does its oxidation of chloride ions not generate hydroxide, but the oxidation actually requires acid for the reaction to occur:^{42,43}



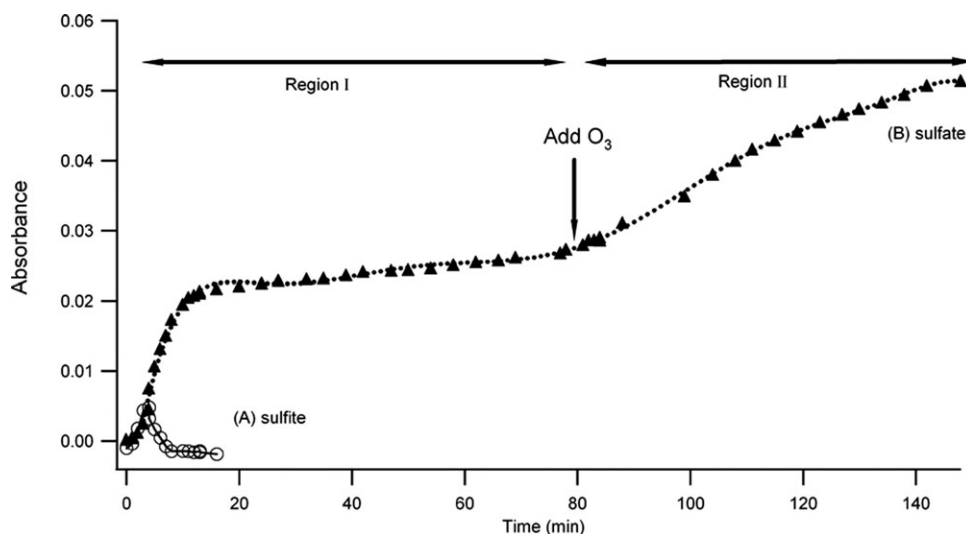


Fig. 4 Time dependence of peaks due to (a) sulfite (open circles) and (b) sulfate (filled triangles) in a typical DRIFTS experiment upon addition of SO_2 ($t = 0$) to an OH-processed $\text{NaCl-MgCl}_2 \cdot 6\text{H}_2\text{O}$ salt sample. The dotted line is a polynomial fit to the data. The sample had been processed with OH for 2 h before the addition of 4.8×10^{15} molecule cm^{-3} SO_2 (region I) at a total pressure of 391 Torr and a relative humidity of 50%. After 80 min, 4.0×10^{16} molecule cm^{-3} O_3 was added and the flows and pumping adjusted to give a total cell pressure of 474 Torr (region II), an SO_2 concentration of 1.3×10^{16} molecule cm^{-3} and a relative humidity of 52%.

However, given the predicted propensity for OH to reside at the interface,^{114–116} some of the OH generated in solution by reactions (5) and (6) will diffuse to the interface, enhancing the interface oxidation and generation of base beyond that expected due to the uptake and reaction of gas phase OH alone.

The relatively rapid disappearance of sulfite and formation of sulfate (Fig. 3) shows that the salt contained an oxidant that was converting sulfite into sulfate in the absence of gaseous O_3 . Region I of Fig. 4 shows the formation and conversion of sulfite to sulfate under these conditions. The rate of sulfate formation decreases substantially after about 10 min, suggesting the oxidant for S(IV) is being depleted as the reaction occurs.

There are a number of species that may be responsible for the initial oxidation of S(IV): residual O_3 , H_2O_2 , and/or HOCl/OCl^- . We consider each of these sequentially.

Residual O_3 oxidation. Because O_3 oxidation of dissolved S(IV) species is the principal pathway for sulfate production in sea salt aerosol under basic conditions, it is possible that residual O_3 dissolved in the liquid film after O_3 photolysis is the oxidizing agent in region I of Fig. 4. To test this hypothesis, a salt sample was exposed to UV light and O_3 for two hours (OH-processing) after which the O_3 flow was turned off, but the UV light exposure continued for another hour. This procedure would have photolyzed residual O_3 . The results obtained upon subsequent exposure to SO_2 were similar to those from the experiments without additional irradiation of the sample. A second experiment was performed in which an OH-processed salt sample was pumped overnight under vacuum prior to addition of SO_2 . There was again no significant change in the oxidation of S(IV) to S(VI). These experiments rule out dissolved ozone as the oxidant in region I.

H_2O_2 oxidation. Hydrogen peroxide is formed from the reaction of HO_2 radicals produced during O_3 photolysis (ESI^\dagger). Hydrogen peroxide is an important oxidizing agent for dissolved SO_2 in aerosols and clouds over a wide range of pH.^{81–85} It is highly soluble in water, with a Henry's law constant¹¹⁷ $H = 8.3 \times 10^4$ M atm⁻¹ and it photolyzes to form two OH radicals with a quantum yield close to unity at 248 and 308 nm.⁴² If H_2O_2 were the oxidizing agent in our experiments, one would expect that additional exposure to UV would photolyze it to generate OH, some of which would diffuse to the aqueous interface, oxidize additional chloride *via* reaction (1) and generate additional hydroxide. This would lead to increased uptake and oxidation of SO_2 . However, the amount of sulfite oxidized in region I did not change significantly upon exposing the sample to UV, so it seems unlikely that the oxidation of sulfite to sulfate was due directly to residual H_2O_2 .

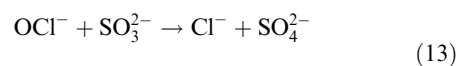
HOCl/OCl^- oxidation. Hypochlorous acid ($\text{p}K_a = 7.53$)¹¹⁸ is formed from the hydrolysis of Cl_2 (produced in reaction (1)). The hydrolysis is fast in the presence of hydroxide ions:



Both HOCl and OCl^- oxidize S(IV) to S(VI).^{88,119–121}



$$k_{12} = 7.6 \times 10^8 \text{ M}^{-1} \text{ s}^{-1}$$



$$k_{13} = 2.3 \times 10^4 \text{ M}^{-1} \text{ s}^{-1}.$$

Aqueous HOCl and OCl^- have been shown to undergo photolysis to produce chlorine atoms.^{122,123} However, chlorine atoms will be converted back to Cl_2 and HOCl/OCl^-

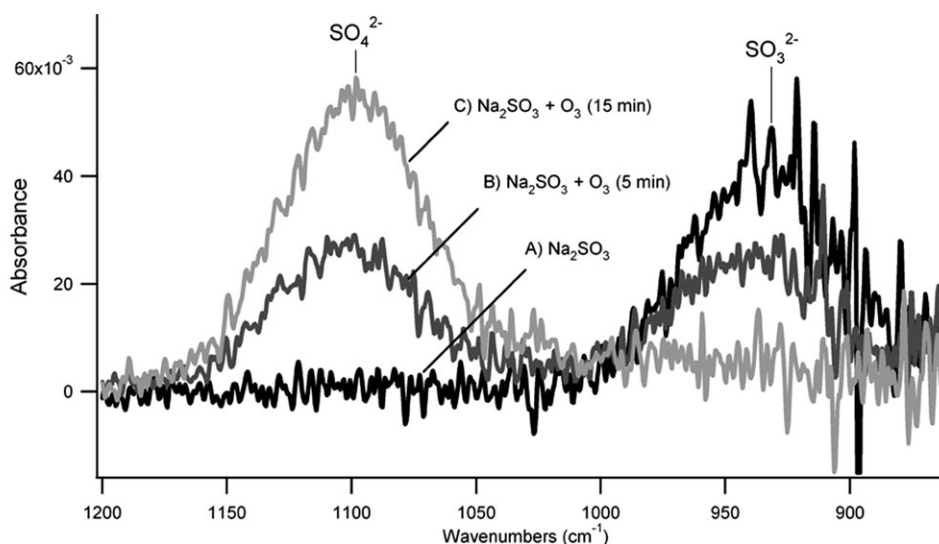


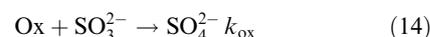
Fig. 5 ATR-FTIR spectra of a bulk solution of 0.70 M Na_2SO_3 before oxidation, after it had been partially oxidized by O_3 and after complete oxidation. These data give the relative infrared absorption cross sections at the peaks for sulfite and sulfate, $\sigma(\text{SO}_3^{2-})/\sigma(\text{SO}_4^{2-}) = 0.8$.

in the presence of high concentrations of Cl^- via reactions (9)–(11). Thus, the results of the post-OH-processing UV exposure suggest that HOCl/OCl^- is the oxidant for S(IV) in region I.

Using the rate constants for reactions (12) and (13), and the $\text{p}K_a$ for HOCl , the relative rate of oxidation of sulfite by HOCl compared to OCl^- is given by $k_{12}[\text{H}^+]/(3.0 \times 10^{-8} k_{13})$. At a pH of 12, this ratio is one, *i.e.* sulfite is oxidized at equal rates by HOCl and OCl^- . At lower pH values, the oxidation by HOCl predominates.

As seen in Fig. 4, the sulfite peak increases rapidly on exposure of the processed salt to gaseous SO_2 and then decreases. This reflects the kinetics of the uptake of SO_2 into the alkaline aqueous film on the salt combined with simultaneous oxidation of the sulfite to sulfate by HOCl/OCl^- . The sulfite concentration at its peak can be estimated in the following manner. The total number of sulfate ions produced at the end of region II was determined by ion chromatography to be 1.3×10^{18} . The infrared absorbance due to sulfite in Fig. 4 can be quantified by measuring the infrared absorption spectrum of a bulk solution of sulfite using ATR-FTIR and then that of the same solution after complete conversion of the sulfite to sulfate. Fig. 5 shows such spectra obtained before, during and after oxidation of a 0.70 M solution of Na_2SO_3 . Using the 1 : 1 relationship between sulfite oxidized and sulfate formed, the absorption cross section for sulfite is found to be 0.8 times that for sulfate. Applying this relationship, along with the calibration of the sulfate infrared absorbance using IC, to the sulfite peak in Fig. 4 gives a total of 1.9×10^{17} sulfite ions in the sample at its peak. If the volume of the aqueous film is 0.04 cm^3 , the sulfite concentration in this aqueous film at its peak is $7.9 \times 10^{-3} \text{ M}$. It should be noted, however, that as the magnesium chloride is converted to the less soluble hydroxide and hydroxychloride, the volume of the aqueous film may shrink. This will lead to the volume of the available solution being overestimated, and hence the sulfite concentration underestimated.

The peak in the sulfite must reflect a balance between uptake of SO_2 and its oxidation in the film and reevaporation, which however is expected to be small for basic solutions. Using a mass accommodation coefficient for SO_2 of 0.11,¹⁰³ the rate of formation of sulfite in a 0.04 cm^3 aqueous film due to uptake of SO_2 at a concentration of $4.8 \times 10^{15} \text{ molecule cm}^{-3}$ is $1.4 \times 10^3 \text{ M s}^{-1}$. This assumes that the film is sufficiently basic so that all of the S(IV) is in the form of sulfite. This is reasonable, given the discussion above and that HSO_3^- was not observed on exposure to SO_2 . The sulfite is simultaneously being removed by an oxidant, Ox:



At the sulfite peak, the rate of uptake must be equal to its rate of removal, *i.e.* $1.4 \times 10^3 \text{ M s}^{-1} = k_{\text{ox}}[\text{Ox}][\text{SO}_3^{2-}] = k_{\text{ox}}[\text{Ox}](7.9 \times 10^{-3} \text{ M})$. If the oxidant is HOCl , $k_{\text{ox}} = 7.6 \times 10^8 \text{ M}^{-1} \text{ s}^{-1}$ and the concentration of HOCl would be $2.3 \times 10^{-4} \text{ M}$. This is an upper limit since the aqueous film volume was assumed to be 0.04 cm^3 . If the oxidant is OCl^- , then $k_{\text{ox}} = 2.3 \times 10^4 \text{ M}^{-1} \text{ s}^{-1}$ and the concentration of OCl^- would be 7.8 M which is unreasonably large. This again suggests that HOCl is the oxidant in region I.

Chamber experiments

Further studies were carried out using an aerosol chamber to verify that the DRIFTS observations are consistent with oxidation of sulfite by HOCl/OCl^- in a liquid film. Fig. 6 shows that while sulfate and sulfite are not observed for NaCl aerosols exposed to SO_2 , sulfate is formed upon addition of gaseous SO_2 to NaOCl aerosols. These experiments cannot be carried out using the DRIFTS apparatus because NaOCl cannot be obtained as a stable solid; it decomposes to O_2 and Cl^- , as well as to higher chlorine oxides, as the solution becomes more concentrated.¹²⁴

Unlike NaOCl aerosols, NaCl aerosols are at a neutral pH. Thus less SO_2 is taken up by NaCl aerosols, and sulfite is

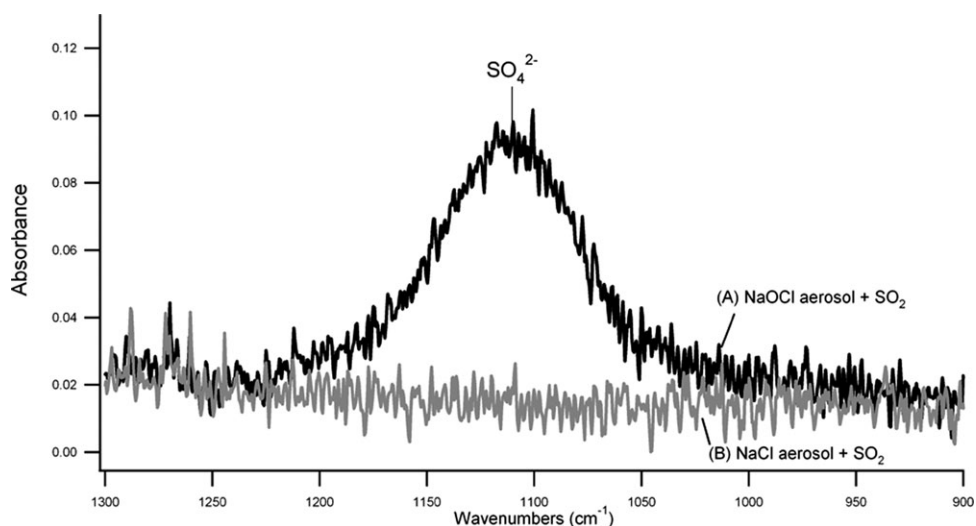


Fig. 6 Long path FTIR aerosol chamber spectra of (a) NaOCl aerosols (black) at 73% RH and 730 Torr after addition of 5×10^{14} molecule cm^{-3} SO_2 ; (b) NaCl aerosols (grey) at 77% RH and 720 Torr, and after addition of 5×10^{14} molecule cm^{-3} SO_2 .

formed in amounts insufficient to be detected by FTIR in our chamber. This observation is consistent with the studies of Hoppel *et al.* who observed the uptake and oxidation of gaseous SO_2 in seawater aerosols but not NaCl aerosols.^{93–95} They attributed this to the rapid acidification of the unbuffered NaCl aerosols which restricted the dissolved S(IV) concentration to $\sim 10 \mu\text{M}$ compared to concentrations that were three orders of magnitude larger in the buffered, alkaline sea-salt particles.

The spectra taken in the aerosol chamber are those of aqueous liquid particles. The fact that they are very similar to those observed using DRIFTS on the reacted $\text{NaCl-Mg}_2\text{Cl}_2 \cdot 6\text{H}_2\text{O}$ samples at 50% RH is further evidence that the chemistry, on what is ostensibly a solid salt mixture in the DRIFTS studies, is actually occurring in a liquid film on the surface. There is a small shift in the position of the sulfate peak, from 1106 cm^{-1} in the DRIFTS experiments (Fig. 3) to 1110 cm^{-1} in the aerosols (Fig. 6). This is consistent with a red-shift observed in the peak of MgSO_4 aerosols as they became more concentrated.¹²⁵

Oxidation of SO_2 by O_3 in region II

After the initial oxidation of S(IV) by HOCl/OCl^- (region I of Fig. 4), the salt was exposed to both O_3 and SO_2 simultaneously at 52% RH. The rate of formation of sulfate again increases (region II), and the total sulfate after one hour determined by IC was 1.3×10^{18} ions, or 2.2×10^{-6} moles. This can be compared to only 6.6×10^{16} sulfate ions formed when the unprocessed salt mixture is exposed to SO_2 for 70 minutes followed by O_3 and SO_2 for 75 minutes in the absence of UV light. This latter amount of sulfate was too small to be observed in the DRIFTS spectra. The fact that significant sulfate formation is observed in region II of the experiment, compared to the control experiment, is an indication that the sample in Fig. 4 must have been basic. At high pH, the oxidation of SO_2 by O_3 is particularly fast due to the high rate constant for the sulfite–ozone reaction.⁸⁷

Further quantitative treatment of the kinetics in this region is not warranted for several reasons. First, as discussed earlier, the volume of the solution on the salt cannot be assumed to be the same as that for the reactant $\text{MgCl}_2 \cdot 6\text{H}_2\text{O}/\text{NaCl}$ mixture once it has been reacted with OH and SO_2 , forming the hydroxide, hydroxychloride and sulfate. In addition, since the aqueous phase in this experiment consists of highly concentrated salt solutions, the Henry's law constants calculated for SO_2 and O_3 based on uptake on water are likely to be upper limits. Furthermore, the kinetics of the dissolution of $\text{Mg}(\text{OH})_2$ and $\text{Mg}_2(\text{OH})_3\text{Cl} \cdot 4\text{H}_2\text{O}$ are not known.

A further complication is the extent to which the DRIFTS technique interrogates the lower levels of the sample. Previous studies using DRIFTS have shown that the IR signal is not restricted to the top few molecular layers of the sample; however, signals from lower portions of the pellet contribute significantly less to the total measured absorbance.³⁶ To examine the extent of the reaction at lower levels of the salt, a depth profile study of SO_4^{2-} within the salt sample was done by IC. After an experiment with an OH processed salt mixture treated similarly to the sample in Fig. 4, the pellet was sliced horizontally into three approximately equal-sized portions. IC analysis showed the presence of sulfate in all three sections. The sulfate represented 0.073, 0.059, and 0.054% by mass of the sample for the top, middle, and bottom sections, respectively. The fact that SO_4^{2-} was present at all depths indicates that the oxidation occurred throughout the sample. However, the DRIFTS spectra at larger extents of reaction, when the upper layers have reacted and changes in the spectra are due to reaction in the lower layers, likely underestimate the total amount of sulfate and hence its rate of formation. Without a detailed understanding of these factors, quantitative treatment of the rate of formation of sulfate due to the ozone oxidation is not reliable.

Despite these uncertainties, it is clear that gaseous OH radicals interact with the salt as if it were a liquid, generating hydroxide *via* the interface reaction (1). This alkalinity leads to the enhanced uptake and oxidation of SO_2 both by

HOCl/OCI⁻ and by O₃. These experiments are qualitatively consistent with the hypothesis of Laskin *et al.*⁴⁰ that the OH interface reaction with Cl⁻ generates alkalinity in the salt which enhances the uptake and oxidation of gaseous SO₂ under laboratory conditions. These experiments were carried out on model sea salt particles in the absence of other sources of acids in air such as HNO₃ which are present in the troposphere. Modeling studies by von Glasow that include the much more complex mixtures found in air suggest that the relative increase in non-sea salt sulfate (nss-SO₄²⁻) when the interface reaction (1) is included is of the order of a few percent or less, depending on the sea salt particle size and the value of the reaction probability.⁷⁰ Part of the reason for this is that in remote regions, the chlorine atoms from the photolysis of Cl₂ generated in reaction (1) react predominantly with methane, forming HCl which can be taken up into the sea salt and titrate part of the alkalinity. In more polluted regions, the production of acids such as HNO₃ can overwhelm the production of hydroxide through the surface reaction.⁵⁵ Measurements of the oxygen isotope composition of sulfate in the Indian Ocean are consistent with the titration of the sea salt alkalinity by a combination of the uptake of gaseous HNO₃ and by the oxidation of dissolved S(IV) by O₃.⁶⁸ The measured ¹⁷O composition of nss-SO₄²⁻ was not well simulated by their model if reaction (1) was assumed to “always maintain(s) an excess of alkalinity”. Reaction (1) would not be expected to maintain such an excess, but rather, to modulate the acidification, so the model predictions in this case may have somewhat overestimated the isotope effect expected in field samples. In any event, while the present experiments qualitatively confirm the impact of OH processing on the uptake and oxidation of SO₂ on model sea salt aerosols under these laboratory conditions, they cannot be directly extrapolated to those found in the troposphere.

4. Summary

The experiments reported here establish that chemistry in thin liquid films on solid salts can be studied using DRIFTS if a small amount of a hygroscopic salt such as magnesium chloride is used in conjunction with a less soluble salt such as NaCl. At a relative humidity which is sufficiently high to deliquesce the first salt, but not high enough to deliquesce the second, a liquid film is formed on the undissolved salt, providing a model for an aqueous salt solution. Using this approach, the reaction of an aqueous chloride film on the NaCl powder with gas phase OH/HO₂ was shown to generate sufficient OH⁻ *via* the interface reaction (1) that sulfite is generated from the uptake of gas phase SO₂ in amounts measurable by DRIFTS. The concurrent oxidation of the sulfite to sulfate occurs *via* the reaction of HOCl/OCI⁻ formed by hydrolysis of the Cl₂ produced simultaneously with the hydroxide ion. The hydroxide formed is expected to be sequestered as Mg(OH)₂ and/or Mg₂(OH)₃Cl·4H₂O, which continues to provide alkalinity to neutralize the acid formed when O₃ oxidizes S(IV) in the thin liquid film. While modeling^{70,126} and field studies^{68,127} suggest that this chemistry is likely to have only a minor impact on the uptake and oxidation of S(IV) in the marine boundary layer under the more

complex conditions of the atmosphere, the experiments reported here show that the chemistry proposed by Laskin *et al.*⁴⁰ involving the uptake and oxidation of S(IV) on OH-processed salt does occur under laboratory conditions.

Acknowledgements

We are grateful to the National Science Foundation (grants #0423804, -0209719 and -0431312) for support of this work. HS thanks the Air & Waste Management Association for a scholarship. We also thank D. Bones for experimental assistance, S. Nickolaissen for instrumental assistance, R. von Glasow and J. N. Pitts Jr. for helpful discussions, and anonymous reviewers for constructive suggestions.

References

- J. T. Jayne, P. Davidovits, D. R. Worsnop, M. S. Zahniser and C. E. Kolb, *J. Phys. Chem.*, 1990, **94**, 6041–6048.
- D. R. Hanson and A. R. Ravishankara, *J. Phys. Chem.*, 1994, **98**, 5728–5735.
- J. H. Hu, Q. Shi, P. Davidovits, D. R. Worsnop, M. S. Zahniser and C. E. Kolb, *J. Phys. Chem.*, 1995, **99**, 8768–8776.
- D. J. Donaldson, J. A. Guest and M. C. Goh, *J. Phys. Chem.*, 1995, **99**, 9313–9315.
- C. George, W. Behnke, V. Scheer, C. Zetzsch, L. Magi, J. L. Ponche and P. Mirabel, *Geophys. Res. Lett.*, 1995, **22**, 1505–1508.
- J. Boniface, Q. Shi, Y. Q. Li, J. L. Cheung, O. V. Rattigan, P. Davidovits, D. R. Worsnop, J. T. Jayne and C. E. Kolb, *J. Phys. Chem. A*, 2000, **104**, 7502–7510.
- E. M. Knipping, M. J. Lakin, K. L. Foster, P. Jungwirth, D. J. Tobais, D. Dabdub and B. J. Finlayson-Pitts, *Science*, 2000, **288**, 301–306.
- S. M. Clegg and J. P. D. Abbatt, *J. Phys. Chem. A*, 2001, **105**, 6630–6636.
- Y. Katrib, G. Deiber, F. Schweitzer, P. Mirabel and C. George, *J. Aerosol Sci.*, 2001, **32**, 893–911.
- R. S. Strekowski, R. Remorov and C. George, *J. Phys. Chem. A*, 2003, **107**, 2497–2504.
- D. J. Gaspar, A. Laskin, W. Wang, S. W. Hunt and B. J. Finlayson-Pitts, *Appl. Surf. Sci.*, 2004, **231–232**, 520–523.
- B. T. Mmerekki and D. J. Donaldson, *J. Phys. Chem. A*, 2003, **107**, 11038–11042.
- P. Davidovits, C. E. Kolb, L. R. Williams, J. T. Jayne and D. R. Worsnop, *Chem. Rev.*, 2006, **106**, 1323–1354.
- K. A. Ramazan, L. M. Wingen, Y. Miller, G. M. Chaban, R. B. Gerber, S. S. Xantheas and B. J. Finlayson-Pitts, *J. Phys. Chem. A*, 2006, **110**, 6886–6897.
- P. Jungwirth, B. J. Finlayson-Pitts and D. J. Tobias, *Chem. Rev.*, 2006, **106**, 1137–1539, Issue on Structure and chemistry at aqueous interfaces.
- B. J. Finlayson-Pitts and J. N. Pitts, Jr., *Chemistry of the Upper and Lower Atmosphere*, Academic Press, San Diego CA, 2000.
- C. E. Kolb, D. R. Worsnop, M. S. Zahniser, P. Davidovits, L. F. Keyser, M.-T. Leu, M. J. Molina, D. R. Hanson, A. R. Ravishankara, L. R. Williams and M. A. Tolbert, in *Progress and Problems in Atmospheric Chemistry*, ed. J. R. Barker, World Scientific, Singapore, 1995, vol. 3, ch. 18.
- C. E. Kolb, J. T. Jayne, D. R. Worsnop and P. Davidovits, *Pure Appl. Chem.*, 1997, **69**, 959–986.
- D. J. Cziczo, J. B. Nowak, J. H. Hu and J. P. D. Abbatt, *J. Geophys. Res.*, [Atmos.], 1997, **102**, 18843–18850.
- D. D. Weis and G. E. Ewing, *J. Geophys. Res.*, [Atmos.], 1999, **104**, 21,275–21,285.
- D. J. Cziczo and J. P. D. Abbatt, *J. Phys. Chem.*, 2000, **104**, 2038–2047.
- R. C. Hoffman, A. L. Laskin and B. J. Finlayson-Pitts, *J. Aerosol Sci.*, 2004, **35**, 869.
- P. H. McMurry and D. R. Rader, *Aerosol Sci. Technol.*, 1985, **4**, 249–268.

- 24 W. C. Hinds, *Aerosol Technology: Properties, Behavior and Measurement of Airborne Particles*, John Wiley and Sons Inc., New York, 1982.
- 25 C. Mund and R. Zellner, *ChemPhysChem*, 2003, **4**, 630–638.
- 26 M. D. King, K. C. Thompson and A. D. Ward, *J. Am. Chem. Soc.*, 2004, **126**, 16710–16711.
- 27 N. Jordanov and R. Zellner, *Phys. Chem. Chem. Phys.*, 2006, **8**, 2759–2764.
- 28 R. C. Sullivan and K. A. Prather, *Anal. Chem.*, 2005, **77**, 3861–3885.
- 29 F. Drewnick, S. S. Hings, P. DeCarlo, J. T. Jayne, M. Gonin, K. Fuhrer, S. Weimer, J. L. Jimenez, K. L. Demerjian, S. Borrmann and D. R. Worsnop, *Aerosol Sci. Technol.*, 2005, **39**, 637–658.
- 30 A. M. Middlebrook, D. M. Murphy, S. H. Lee, D. S. Thomson, K. A. Prather, R. J. Wenzel, D. Y. Liu, D. J. Phares, K. P. Rhoads, A. S. Wexler, M. V. Johnston, J. L. Jimenez, J. T. Jayne, D. R. Worsnop, I. Yourshaw, J. H. Seinfeld and R. C. Flagan, *J. Geophys. Res.*, [Atmos.], 2003, **108**, DOI: 10.1029/2001JD000660.
- 31 D. Y. H. Pui, R. C. Flagan, S. L. Kaufman, A. D. Maynard, J. F. de la Mora, S. V. Hering, J. L. Jimenez, K. A. Prather, A. S. Wexler and P. J. Ziemann, *J. Nanopart. Res.*, 2004, **6**, 314–315.
- 32 D. G. Nash, X. F. Liu, E. R. Mysak and T. Baer, *Int. J. Mass Spectrom.*, 2005, **241**, 89–97.
- 33 D. J. Cziczko, D. M. Murphy, P. K. Hudson and D. S. Thomson, *J. Geophys. Res.*, [Atmos.], 2004, **109**, DOI: 10.1029/2003JD004032.
- 34 N. Takegawa, Y. Miyazaki, Y. Kondo, Y. Komazaki, T. Miyakawa, J. L. Jimenez, J. T. Jayne, D. R. Worsnop, J. D. Allan and R. J. Weber, *Aerosol Sci. Technol.*, 2005, **39**, 760–770.
- 35 P. R. Griffiths and M. P. Fuller, in *Advances in Infrared and Raman Spectroscopy*, ed. R. J. H. Clark and R. H. Hester, Heyden and Sons, London, Editon edn, 1982, vol. 9, pp. 63–129.
- 36 R. Vogt and B. J. Finlayson-Pitts, *J. Phys. Chem.*, 1994, **98**, 3747–3755.
- 37 M. Ullerstam, M. S. Johnson, R. Vogt and E. Ljungstrom, *Atmos. Chem. Phys.*, 2003, **3**, 2043–2051.
- 38 S. Langer, R. S. Pemberton and B. J. Finlayson-Pitts, *J. Phys. Chem. A*, 1997, **101**, 1277–1268.
- 39 K. W. Oum, M. J. Lakin, O. Dehaan, T. Brauers and B. J. Finlayson-Pitts, *Science*, 1998, **279**, 74–77.
- 40 A. Laskin, D. J. Gaspar, W. Wang, S. W. Hunt, J. P. Cowin, S. D. Colson and B. J. Finlayson-Pitts, *Science*, 2003, **301**, 340–344.
- 41 B. J. Finlayson-Pitts, *Chem. Rev.*, 2003, **103**, 4801–4822.
- 42 J. R. Barker and X. Yu, *J. Phys. Chem. A*, 2003, **33**, 747–763.
- 43 X. Yu, *J. Phys. Chem. Ref. Data*, 2004, **33**, 747–763.
- 44 A. Laskin, H. Wang, W. H. Robertson, J. P. Cowin, M. J. Ezell and B. J. Finlayson-Pitts, *J. Phys. Chem. A*, 2006, **110**, 10619–10627.
- 45 A. H. Woodcock, *J. Meteorol.*, 1953, **10**, 362–371.
- 46 A. H. Woodcock, *J. Geophys. Res.*, [Atmos.], 1972, **77**, 5316–5321.
- 47 D. C. Blanchard, *J. Geophys. Res.*, [Atmos.], 1985, **90**, 961–963.
- 48 D. Hitchcock, L. L. Spiller and W. E. Wilson, *Atmos. Environ.*, 1980, **14**, 165–182.
- 49 M. O. Andreae, R. J. Charlson, F. Bruynseels, H. Storms, R. Van Grieken and W. Maenhaut, *Science*, 1986, **232**, 1620–1623.
- 50 W. C. Keene, A. Pszenny, D. J. Jacob, R. A. Duce, J. N. Galloway, J. J. Schultz-Tokos, H. Sievering and J. Boatman, *Global Biogeochem. Cycles*, 1990, **4**, 407–430.
- 51 H. Sievering, J. Boatman, J. N. Galloway, W. Keene, Y. Kim, M. Luria and J. Ray, *Atmos. Environ.*, 1991, **25A**, 1479–1487.
- 52 H. Sievering, J. Boatman, E. Gorman, Y. Kim, L. Anderson, G. Ennis, M. Luria and S. Pandis, *Nature*, 1992, **360**, 571–574.
- 53 W. L. Chameides and A. W. Stelson, *J. Geophys. Res.*, [Atmos.], 1992, **97**, 20,565–520,580.
- 54 W. L. Chameides and A. W. Stelson, *J. Geophys. Res.*, [Atmos.], 1993, **98**, 9051–9054.
- 55 W. Keene, D. J. Jacob, A. A. P. Pszenny, R. A. Duce, J. J. Schultz-Tokos and J. N. Galloway, *J. Geophys. Res.*, [Atmos.], 1993, **98**, 9047–9049.
- 56 L. M. McInnes, D. S. Covert, P. K. Quinn and M. S. Germani, *J. Geophys. Res.*, [Atmos.], 1994, **99**, 8257–8268.
- 57 H. Sievering, E. Gorman, T. Ley, A. Pszenny, M. Springer-Young, J. Boatman, Y. Kim, C. Nagamoto and D. Wellman, *J. Geophys. Res.*, [Atmos.], 1995, **100**, 23075–23081.
- 58 M. Posfai, J. R. Anderson, P. R. Buseck and H. Sievering, *J. Geophys. Res.*, [Atmos.], 1995, **100**, 23063–23074.
- 59 C. C. O'Dowd, M. H. Smith, I. E. Consterdine and J. A. Lowe, *Atmos. Environ.*, 1997, **31**, 73–80.
- 60 W. C. Keene, R. Sander, A. A. P. Pszenny, R. Vogt, P. J. Crutzen and J. N. Galloway, *J. Aerosol Sci.*, 1998, **29**, 339–356.
- 61 V. Kerminen, K. Teinila, R. Hillamo and T. Pakkanen, *J. Aerosol Sci.*, 1998, **29**, 929–942.
- 62 C. Gurciullo, B. Lerner, H. Sievering and S. N. Pandis, *J. Geophys. Res.*, [Atmos.], 1999, **104**, 21719–721731.
- 63 G. P. Ayers, R. W. Gillet, J. M. Caaney and A. L. Dick, *J. Atmos. Chem.*, 1999, **33**, 299–319.
- 64 D. Katoshevski, A. Nenes and J. H. Seinfeld, *J. Aerosol Sci.*, 1999, **30**, 503–532.
- 65 A. van de Berg, F. Dentener and J. Lelieveld, *J. Geophys. Res.*, [Atmos.], 2000, **105**, 11,671–611,698.
- 66 S. L. Gong and L. A. Barrie, *J. Geophys. Res.*, [Atmos.], 2003, **108**, DOI: 10.1029/2002JD003181.
- 67 A. Virkkula, K. Teinila, R. Hillam, V. Kerminen, S. Saarikoski, M. Aurela, I. K. Koponen and M. Kulmala, *J. Geophys. Res.*, [Atmos.], 2006, **111**, DOI: 10.1029/2004JD004958.
- 68 B. Alexander, R. J. Park, D. J. Jacob, Q. B. Li and R. M. Yantoca, *J. Geophys. Res.*, [Atmos.], 2005, **110**, DOI: 10.1029/2004JD005659.
- 69 H. Sievering, B. Lerner, J. Slavich and Anderson, *J. Geophys. Res.*, [Atmos.], 1999, **104**, 21707–721717.
- 70 R. von Glasow, *Atmos. Chem. Phys. Discuss.*, 2006, **6**, 3657–2685.
- 71 R. von Glasow and R. Sander, *J. Geophys. Res.*, [Atmos.], 2002, **107**, DOI: 10.1029/2001JD000943.
- 72 H. Sievering, J. Caaney, M. Harvey, J. McGregor and S. Nichol, *J. Geophys. Res.*, [Atmos.], 2004, **109**, DOI: 10.1029/2003JD004315.
- 73 R. Sander and P. J. Crutzen, *J. Geophys. Res.*, [Atmos.], 1996, **101**, 9121–9138.
- 74 R. J. Charlson, J. E. Lovelock, M. O. Andreae and S. G. Warren, *Nature*, 1987, **326**, 655–661.
- 75 J. T. Houghton, Y. Ding, D. J. Griggs, M. Noguera, P. J. van der Linden, X. Dai, K. Maskell and C. A. Johnson, *Climate Change 2001: The Scientific Basis*, Cambridge University Press, Cambridge, 2001.
- 76 J. E. Penner, S. Y. Zhang, M. Chin, C. C. Chaung, J. Feichter, Y. Feng, I. V. Geogdzhayev, P. Ginoux, M. Herzog, A. Higurashi, D. Koch, C. Land, U. Lohmann, M. Mishchenko, T. Nakajima, G. Pitari, B. S. Tegen and L. Stowe, *J. Atmos. Sci.*, 2002, **59**, 441–460.
- 77 S. E. Schwartz, *J. Air Waste Manage. Assoc.*, 2004, **54**, 1351–1359.
- 78 N. Bell, D. Koch and D. T. Shindell, *J. Geophys. Res.*, [Atmos.], 2005, **110**, DOI: 10.1029/2004JD005538.
- 79 J. Haywood and O. Boucher, *Rev. Geophys.*, 2000, **38**, 513–543.
- 80 G. H. Sillen and A. E. Martell, *Stability Constants of Metal-Ion Complexes*, Chemical Society, London, 1964.
- 81 M. R. Hoffman and J. O. Edwards, *J. Phys. Chem.*, 1975, **79**, 2096–2098.
- 82 S. A. Penkett, M. R. Jones, K. A. Brice and A. E. J. Eggleton, *Atmos. Environ.*, 1978, **13**, 123–137.
- 83 R. L. Martin and D. E. Damschen, *Atmos. Environ.*, 1981, **15**, 1615–1621.
- 84 J. Lagrange, C. Pallares, G. Wenger and P. L'Arange, *Atmos. Environ.*, 1996, **30**, 1038–1018.
- 85 J. A. Lind, A. L. Lazrus and G. L. Kok, *J. Geophys. Res.*, [Atmos.], 1987, **92**, 4171–4177.
- 86 Y.-N. Lee, J. Shen, P. J. Klotz, S. E. Schwartz and L. Newman, *J. Geophys. Res.*, [Atmos.], 1986, **91**, 13264–13274.
- 87 M. R. Hoffman, *Atmos. Environ.*, 1986, **20**, 1145–1154.
- 88 R. Vogt, P. J. Crutzen and R. Sander, *Nature*, 1996, **383**, 327–330.
- 89 P. K. Dasgupta, P. A. Mitchell and W. W. Philip, *Atmos. Environ.*, 1979, **13**, 775–782.
- 90 A. G. Clarke and M. Radojevic, *Atmos. Environ.*, 1983, **17**, 617–624.
- 91 A. G. Clarke and M. Radojevic, *Atmos. Environ.*, 1984, **18**, 2761–2767.

- 92 J. Z. Zhang and F. J. Millero, *Geochim. Cosmochim. Acta*, 1991, **55**, 677–685.
- 93 P. Caffrey, W. Hoppel, G. Frick, F. James, N. Shantz, W. R. Leatch, L. Pasternack, T. Albrechcinski and J. Ambrusko, *J. Geophys. Res., [Atmos.]*, 2001, **106**, 27,635–627,645.
- 94 W. A. Hoppel, L. Pasternack, P. Caffrey, G. Frick, J. Fitzgerald, D. Hegg, S. Gao, J. Ambrusko and T. Albrechcinski, *J. Geophys. Res., [Atmos.]*, 2001, **106**, 27575–527585.
- 95 W. A. Hoppel and P. F. Caffrey, *J. Geophys. Res., [Atmos.]*, 2005, **110**, DOI: 10.1029/2005JD006239.
- 96 W. R. Stockwell and J. G. Calvert, *Atmos. Environ.*, 1983, **17**, 2231–2235.
- 97 I. N. Tang, *J. Aerosol Sci.*, 1976, **7**, 361–371.
- 98 R. Vogt and B. J. Finlayson-Pitts, *J. Phys. Chem.*, 1995, **99**, 17269–17272.
- 99 D. R. Kester, I. W. Duedall, D. N. Connors and R. M. Pytkowicz, *Limnol. Oceanogr.*, 1967, **12**, 176–179.
- 100 G. J. Kipouros and D. R. Sadoway, *J. Light Metals*, 2001, **1**, 111–117.
- 101 F. H. Herbstein, M. Kapon and A. Weissman, *Isr. J. Chem.*, 1982, **22**, 207–213.
- 102 W. Braun, J. T. Herron and D. K. Kahaner, *Int. J. Chem. Kinet.*, 1988, **20**, 51–62.
- 103 S. P. Sander, R. R. Friedl, D. M. Golden, M. J. Kurylo, G. K. Moortgat, H. Keller-Rudek, W. P. H., A. R. Ravishankara, C. E. Kolb, M. J. Molina, B. J. Finlayson-Pitts, R. E. Huie and V. L. Orkin, *Chemical Kinetics and Photochemical Data for Use in Atmospheric Studies. Evaluation no. 15*, Jet Propulsion Laboratory, California Institute of Technology, Pasadena, 2006.
- 104 R. Atkinson, R. A. Cox, J. N. Crowley, J. R. F. Hampson, R. G. Hynes and M. E. Jenkin, <http://www.iupac-kinetic.ch.cam.ac.uk/>, 2006.
- 105 J. U. White, *J. Opt. Soc. Am.*, 1942, **32**, 285–288.
- 106 R. A. Robinson and R. H. Stokes, *Electrolyte Solutions*, 2nd edn, Butterworths, London, 1959.
- 107 B. L. Wedzicha, I. R. Bellion and S. J. Goddard, *Food Chem.*, 1992, **44**, 165–171.
- 108 C. L. Aardahl and E. J. Davis, *Appl. Spectrosc.*, 1996, **50**, 71–77.
- 109 M. Altmaier, V. Metz, V. Neck, R. Müller and Th. Fanghänel, *Geochim. Cosmochim. Acta*, 2003, **67**, 3595–3601.
- 110 M. W. Bodine, Jr., *Geology*, 1976, **4**, 76–80.
- 111 C. Mažuranic, H. Bilinski and B. Matkovic, *J. Am. Ceram. Soc.*, 1982, **65**, 523–526.
- 112 R. Sander, <http://www.mpch-mainz.mpg.de/~sander/res/henry.html>.
- 113 K. Sehested, J. Holcman and E. J. Hart, *J. Phys. Chem.*, 1983, **87**, 1951–1954.
- 114 M. Roeselova, P. Jungwirth, D. J. Tobais and R. B. Gerber, *J. Phys. Chem. B*, 2003, **107**, 12690–12699.
- 115 M. Roeselová, J. Vieceli, L. X. Dang, B. C. Garrett and D. J. Tobias, *J. Am. Chem. Soc.*, 2004, **126**, 16308–16309.
- 116 R. Vácha, P. Slavicek, M. Mucha, B. J. Finlayson-Pitts and P. Jungwirth, *J. Phys. Chem. A*, 2004, **108**, 11573–11579.
- 117 D. W. O'Sullivan, M. Lee, B. C. Noone and B. G. Heikes, *J. Phys. Chem.*, 1996, **100**, 3241–3247.
- 118 D. R. Lide, *Handbook of Chemistry and Physics*, 74 edn, CRC Press, Boca Raton, FL, 1994.
- 119 K. D. Fogelman, D. M. Walker and D. W. Margerum, *Inorg. Chem.*, 1989, **28**, 986–993.
- 120 B. S. Yiin and D. W. Margerum, *Inorg. Chem.*, 1988, **27**, 1670–1672.
- 121 R. D. Srivastava, P. C. Nigam and S. K. Goyal, *Ind. Eng. Chem. Fundam.*, 1980, **19**, 207–209.
- 122 C. L. Thomsen, D. Madsen, J. A. Poulsen, J. Thogersen, S. J. K. Jensen and S. R. Keiding, *J. Chem. Phys.*, 2001, **115**, 9361–9369.
- 123 M. Lim, S. Gnanakaran and R. M. Hochstrasser, *J. Chem. Phys.*, 1997, **106**, 3485–3493.
- 124 J. W. Mellor, *A Comprehensive Treatise on Inorganic and Theoretical Chemistry*, Longmans, Green and Co. Ltd., London, 1946.
- 125 L. J. Zhao, Y. H. Zhang and Z. F. Wei, *J. Phys. Chem. A*, 2006, **110**, 951–958.
- 126 R. Sander, P. J. Crutzen and R. von Glasow, *Science*, 2004, **303**, 628c.
- 127 W. C. Keene and A. A. P. Pszenny, *Science*, 2004, **303**.